

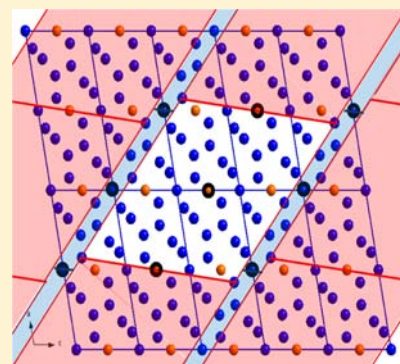
Incommensurately Modulated  $\delta''$ - $\text{Au}_{1+x}\text{Cd}_{2-x}$  Formed by an Unquenchable Phase Transformation from the  $\gamma$ -Brass  $\delta'$ -Phase

Partha P. Jana\* and Sven Lidin

CAS Chemical Centre, Lund University, Getingevägen 60, Box 124, Lund SE-22100, Sweden

## Supporting Information

**ABSTRACT:** The synthesis and structural determination of the compound  $\delta''$ - $\text{Au}_{1+x}\text{Cd}_{2-x}$  ( $0.07 \leq x \leq 0.08$ ) is reported. The structure may be formally derived from that of  $\xi$ - $\text{CoZn}_{13}$ , but elemental ordering causes an incommensurate modulation as determined by single-crystal X-ray diffraction at room temperature. The compound  $\delta''$ - $\text{Au}_{3.23}\text{Cd}_{5.76}$  crystallizes in the monoclinic super space group  $C2/m(0\beta^1/2)00$  with lattice parameters  $a = 14.790(2)$  Å,  $b = 8.251(1)$  Å,  $c = 12.744(1)$  Å,  $\beta = 115.182(9)^\circ$  and a q-vector  $q = (0\beta^1/2)$ ,  $\beta = 0.579b^*$ . The  $\delta''$ -phase is stable up to 652(1) K.



## INTRODUCTION

Intermetallic compounds or alloys have broad industrial applications and richly varied structural chemistry, and physical properties (electronic, magnetic, thermal, and mechanical).<sup>1–8</sup> From the very beginning of civilization, the properties of the metals and the intermetallic compounds have been extensively used. These materials were always associated with human culture. In the past 20 years a large number of intermetallics have been synthesized and characterized. Their study has provided much information about their structure–property relationships. The intermetallic phases presently attract most attention because of their structural complexity and challenge the understanding of the underlying stabilization mechanism.<sup>9,10</sup> In recent years, the origin of some large intermetallic structures have become clear within the framework of complex intermetallics (CMA), quasicrystals (QCs) and quasicrystalline approximants. Nevertheless, many binary complex intermetallic structures formed between the elements of Group 11 and Group 12 in the periodic table are yet to be uncovered. We concentrate in this report on a new Au–Cd binary phase.

Gold–cadmium alloys have been found to be used as Shape Memory Alloys (SMA).<sup>11–16</sup> The shape memory effect (SMA) in the Au–Cd alloys is caused by the martensitic transformation and its reverse transformation.<sup>17–20</sup> Several modifications of martensite structure at low temperature from the  $\beta$ -brass type phase of the Au–Cd alloy have been observed at about 47.5–50 atom percent of cadmium.<sup>21–23</sup> The  $\delta$ -phase field in the Au–Cd system deserves chemical interest because of its allotropic transformations. The  $\delta$ -phase region of Au–Cd extends from 578 K, the lower stability boundary of  $\delta''$  to a maximum temperature of about 833 K for Au rich  $\delta$ -phase, and the composition ranges from  $\sim 33$  to  $\sim 38$  atomic percent of gold.<sup>24</sup> The construction of  $\delta$ - and  $\delta'$ -phase boundaries in the

phase diagram has been assessed and composed by experimental data from various sources.<sup>24–26</sup> According to previous reports the  $\delta$ - and  $\delta'$ -phases correspond to the  $\gamma$ -brass type phase.<sup>24</sup> The structure of the  $\delta''$ -phase is unknown till to date (Figure 1), and the transformation from  $\delta'$  to  $\delta''$  is reconstructive as can be seen by the large, discontinuous changes in the powder pattern recorded in real time during cooling.<sup>24</sup>

From this background, we reinvestigated the region around  $\text{Au}_{30}\text{Cd}_{70}$  in the cadmium rich part of the Au–Cd system. Samples with nominal composition ranging from 29 to 38 atomic percent of gold were synthesized. In this paper, we report on the existence, homogeneity range, thermal stability, and complete crystal structure of  $\delta''$ - $\text{Au}_{1+x}\text{Cd}_{2-x}$  ( $0.07 \leq x \leq 0.08$ ) and its relation to the  $\xi$ - $\text{CoZn}_{13}$ <sup>27</sup> structure.

## EXPERIMENTAL SECTION

**Synthesis.** Single-phase samples with nominal composition  $x_{\text{Au}} = 0.29, 0.31, 0.33, 0.35,$  and  $0.38$  were synthesized by conventional solid state techniques. The preparations were carried out on a 0.3 g scale from elemental gold (99.99%, JM) and cadmium (99.99%, Chempur) in previously outgassed, evacuated quartz glass ampules (3 cm long, 0.8 cm in diameter). The metals were heated up to 973 K (at a rate of  $135 \text{ K h}^{-1}$ ) and were kept at this temperature for 12 h. Hereafter, the temperature was reduced to 773 K at a rate of  $3.15 \text{ K h}^{-1}$  and annealed at this temperature over the course of 4 days after which the ampules were cooled to room temperature over the period of 12 h. The synthesis procedure involves heating the sample to achieve a melt and then anneal anywhere in the  $\delta$  region ( $\delta'$  or  $\delta''$ ). Annealing is followed by quenching to room temperature. Regardless of annealing temperature, in each synthesis the phase produced is  $\delta''$ . This

Received: June 3, 2013

Published: October 28, 2013

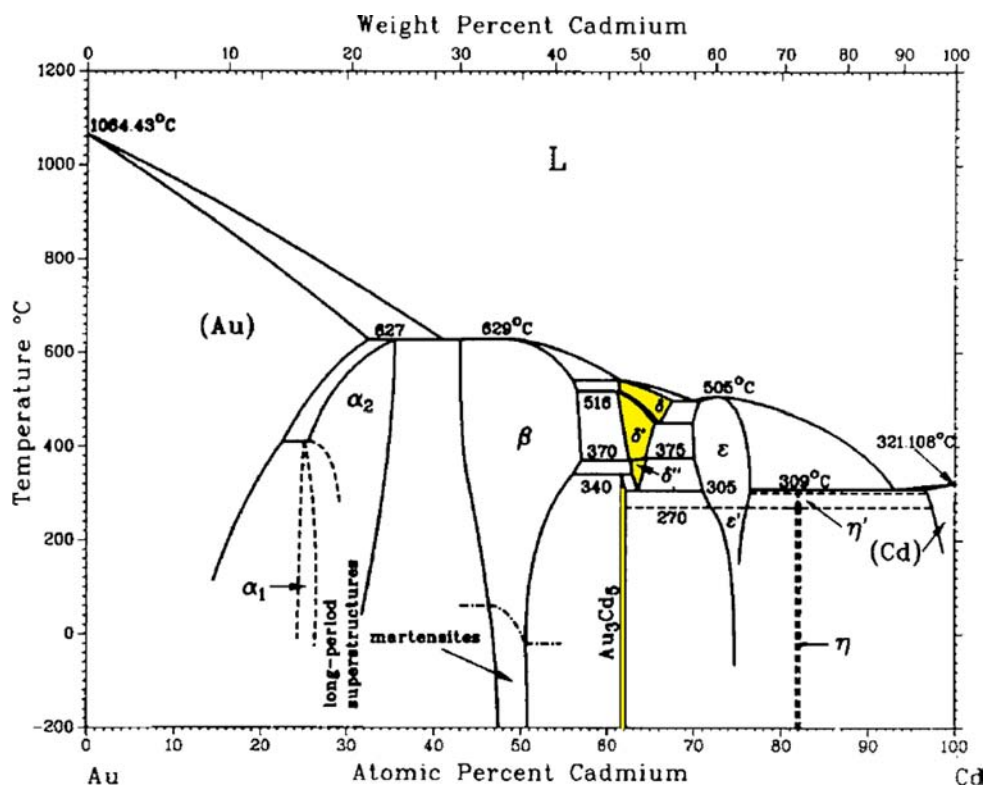


**Figure 1.** Au–Cd phase diagram (Bulletin of Alloy Phase Diagrams Vol. 7, No. 1, 1986.). Reprinted with permission from Okamoto, H; Massalski, T. B., Eds.; *Phase diagrams of binary gold alloys*; ASM International: Metals Park, OH, 1986. Copyright 1986 ASM International.

indicates that the  $\delta$  and  $\delta'$  phases undergo unquenchable phase transformations to  $\delta''$  on cooling. Products obtained from these reactions were silvery, brittle, and stable in air.

**Characterization.** Products were characterized by X-ray diffraction methods as well as energy dispersive X-ray spectroscopy (EDS).

X-ray powder diffraction experiments were performed in transmission mode on a Stoe Stadi MP (vertical setup), equipped with a curved germanium monochromator (Johansson geometry) and a MYTHEN detector, using  $\text{Cu}_{K\alpha 1}$  radiation. JANA2006 package program<sup>28</sup> was used for Rietveld refinements on single phase samples.

To get reliable information about the cadmium-rich monoclinic phase and their homogeneity range, five single crystals from different loaded composition were studied at room temperature by means of single crystal X-ray diffraction. Suitable crystals were picked from the crushed sample and mounted on a silica fiber. The diffraction intensities were measured at room temperature with a four circle diffractometer (X-calibur, Eos) equipped with graphite monochromatized  $\text{Mo}_{K\alpha}$  ( $\lambda = 0.71073 \text{ \AA}$ ) radiation. The program suite CrysAlisPro20 was used for data reduction and integration. Jana2006<sup>28,29</sup> package program was used for the structure solution and refinement.

Diffraction patterns from X-ray single crystal experiments show strong main reflections and weak satellite reflections, clearly indicating a modulated structure. In one-dimensional (1D) modulated structures the reciprocal space vectors are generally expressed as  $H = ha^* + kb^* + lc^* + mq_1$  (where,  $a^*$ ,  $b^*$ , and  $c^*$  are the basis vectors of the three-dimensional (3D) reciprocal lattice and  $h$ ,  $k$ , and  $l$  are the 3D Miller indices and  $m$  is an additional Miller index). The modulation vector  $q_1$  is expressed as  $q_1 = \alpha_i a^* + \beta_j b^* + \gamma_l c^*$ ; where  $\alpha_i$ ,  $\beta_j$ , and  $\gamma_l$  are numbers which are irrational for incommensurate modulations. The number of modulation vectors defines the modulation dimension. The modulations in general come from a displacement of the atoms (displacive modulation), a change of the occupation probability (occupation modulation), or from a variation of temperature factors for an atomic species. Fluctuation of the atomic positions from the average structure as well as the variation of interatomic distances can be visualized as a function of an additional parameter  $t$ . This corresponds to a variation

of the phase of the modulation. Because all distances and displacements which occur within a structure are periodic functions of  $t$ , the total information can be stated by values within the interval  $0 \leq t \leq 1$ .<sup>10</sup>

The compositions of selected specimens were examined in a scanning electron microscope (a JEOL 3000 with a secondary electron (SEI) detector) providing an energy dispersive X-ray spectrometer (EDS). EDS spectra were recorded from those samples which had been previously studied by single crystal X-ray diffraction experiments. No impurities of elements heavier than carbon were detected to be present in the selected specimens. The thermo-chemical properties of two samples,  $\text{Au}_{3.23}\text{Cd}_{5.76}$  (C2) and  $\text{Au}_{3.22}\text{Cd}_{5.78}$  (C3), were studied in the temperature range 300–1373 K employing a differential scanning calorimeter (DSC, NETZSCH Instrument: STA449 F3 jupiter). Usually 30–40 mg powder samples were placed into small alumina crucibles. An empty crucible of similar size was used as a reference. The experiments were carried out under nitrogen atmosphere. To ensure reproducibility of the thermal events the experiments were usually repeated twice at heating and cooling rates of  $10 \text{ K min}^{-1}$ .

## RESULTS

**Phase Analysis.** The homogeneity range of monoclinic  $\delta''$ - $\text{Au}_{1+x}\text{Cd}_{2-x}$  ( $0.07 \leq x \leq 0.08$ ) was studied by means of preparative methods, calorimetric measurements, X-ray diffraction, and EDS analyses. Chemical compositions determined by EDS are essentially in accord with the compositions determined by the single crystal X-ray structure refinement. The phase exhibits a very narrow homogeneity range extending from  $\text{Au}_{3.25}\text{Cd}_{5.75}$  to  $\text{Au}_{3.22}\text{Cd}_{5.78}$ . The loaded compositions for different preparation, the corresponding refined compositions from single crystal X-ray diffraction experiments, and EDS analyses for selected crystalline specimens can be found in the Supporting Information. The sample with nominal composition  $x_{\text{Au}} = 0.29$  exclusively form  $\text{Cu}_3\text{P}$ -type binary adjacent  $\epsilon$ - $\text{AuCd}_3$ <sup>23</sup> (space group  $P6_3cm$  (185),  $a = 8.163(1) \text{ \AA}$ ,  $c =$

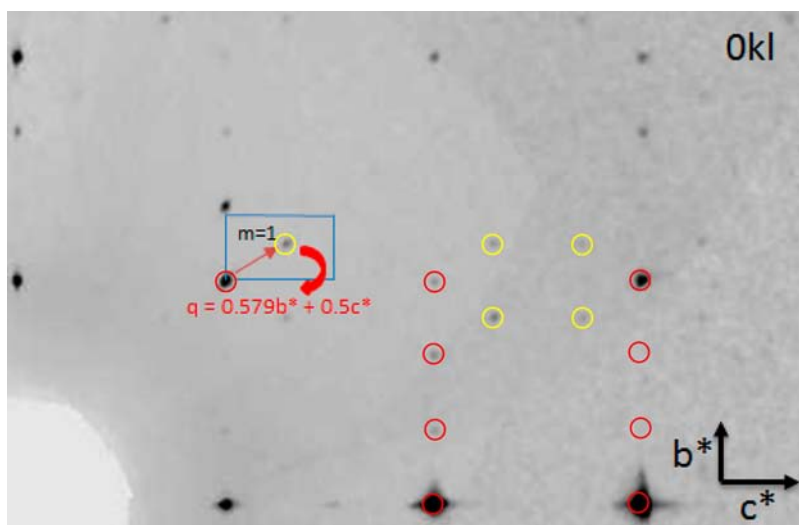


**Figure 2.** Reconstruction of reciprocal space plane (0kl) (in monoclinic setting) of C2. Main reflections are indicated by red circles. The weak satellites (yellow circles) can be indexed by a single  $q$  vector, i.e.,  $q = 0.579b^* + 0.5c^*$ .

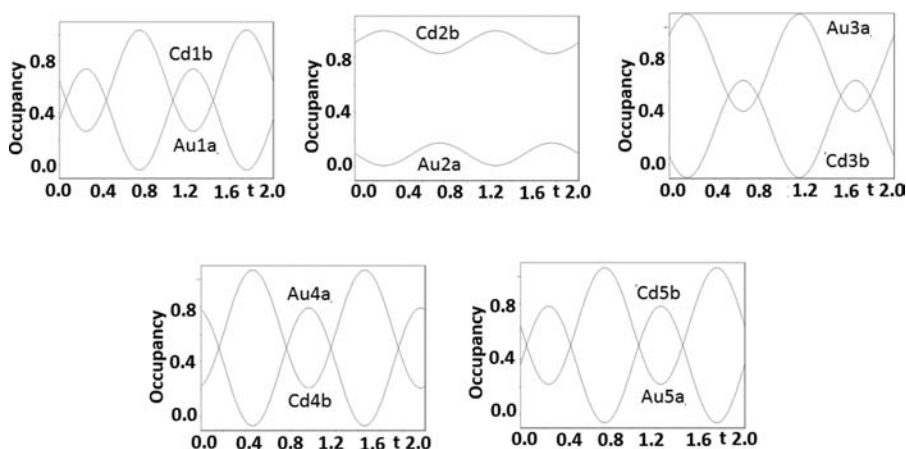


**Figure 3.** Representation of the occupancy modulation behavior between Au and Cd on various atomic sites in the  $Au_{3.22}Cd_{5.78}$ . Note the total occupancy is constant (unity) but that the relative contribution to a given site (Cd/Au balance) varies with  $t$ , i.e., with respect to position relative to an absolute origin in the crystal.

8.552(2) Å) as observed by EDS analysis and X-ray diffraction experiments. Specimen with  $x_{Au} = 0.37$  shows the existence of  $W_5Si_3$  type  $Au_3Cd_5$  (space group =  $I4/mcm$  (140),  $a = 10.745(1)$  Å,  $c = 5.357(7)$  Å). Single crystal X-ray structure determination and EDS analyses are essentially in accord with the previously postulated composition- $Au_3Cd_5$ .<sup>24</sup>

Phase pure  $Au_{1+x}Cd_{2-x}$  can be synthesized between the two extreme compositions as shown by a Rietveld refinement<sup>28,30,31</sup> performed on a sample with  $x_{Au} = 0.36$ . Positional parameters of the average structure determined from single crystal X-ray diffraction data were used as starting parameters for the refinements against X-ray diffraction data of powder sample. A profile fit is given in the Supporting Information, Figure S1. Thermal analyses show that the  $\delta''$ -phase transforms at 652(1) K (peak maxima; onset: 651(2) K). Recrystallization of  $\delta''$ - $Au_{1+x}Cd_{2-x}$  appears to be kinetically inhibited at the chosen cooling rate of 10 K  $min^{-1}$ . It is noted that the phase transition temperatures for the various specimens did not differ significantly.

**Modulated Structure. Structural Solution.** The diffraction pattern is monoclinic and follows a C-centered lattice. The data sets were averaged in the point group  $2/m$ . For the average cell

(Figure 2), the diffraction pattern indicates the cell parameters  $a = 14.790(2)$  Å,  $b = 8.251(1)$  Å,  $c = 12.744(1)$  Å,  $\beta = 115.182(9)^\circ$  for C2. Systematic absences for main reflections indicate the space group is  $C2/m$ . Additional satellite reflections indicate a superstructure along the [011] direction. The satellite reflections could be indexed by the incommensurate  $q$  vector  $q = (0\beta^{1/2})$ ,  $\beta = 0.579b^*$ . No additional systematic absences indicating translational components of the symmetry operations along the fourth dimension could be detected and hence, the highest (3 + 1)D superspace group symmetry allowed is  $C2/m(0\beta^{1/2})00$ . Only first order satellites were detected with the criteria for observed reflections ( $I > 3\sigma(I)$ ). For the structural solution and refinement, the Jana2006 program package<sup>28</sup> was used.

The structure solution generated 14 atomic positions in the asymmetric unit. Extinction correction, anisotropic displacement parameters, and positional modulations of all the atomic positions were applied at this stage. The refinement converged to  $R_{obs} = 14\%$  for all observed reflections ( $R_{obs} = 7\%$  for main reflections and  $R_{obs} = 40\%$  for first order satellites). Analysis of the Debye–Waller factors suggested mixed occupancy for five positions (M1–M5), and those were subsequently modeled

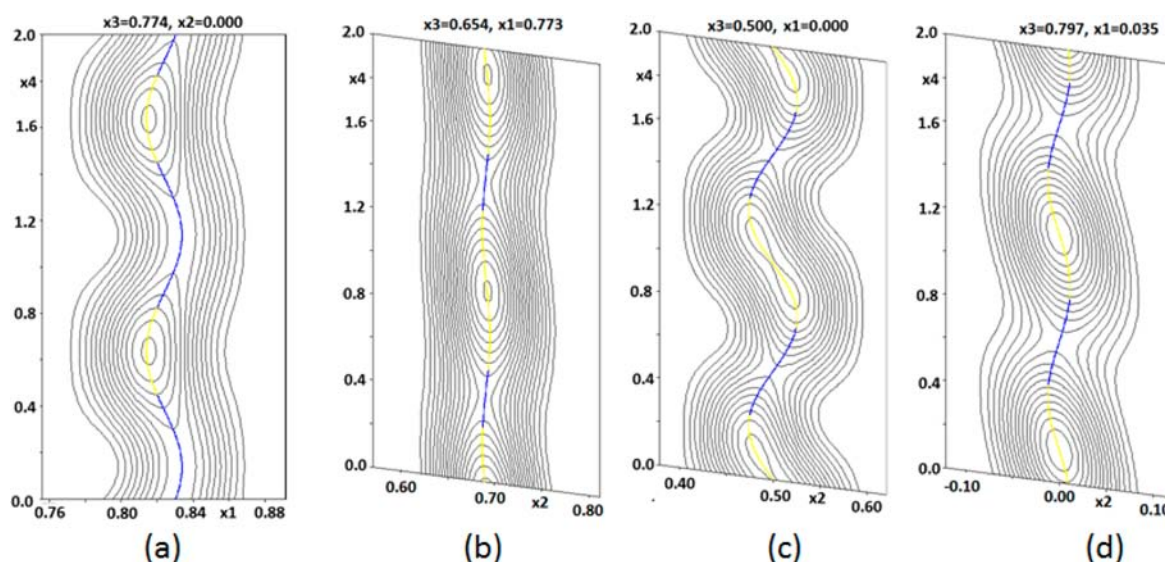


**Figure 4.** Electron density maps of the Au1a/Cd1b (a), Au3a/Cd3b (b), Au4a/Cd4b (c), and Au5a/Cd5b (d), respectively in the  $\text{Au}_{3.22}\text{Cd}_{5.78}$  calculated from  $F(\text{obs})$ . The colored lines represent the refined modulation behavior of the Au (yellow) and Cd (blue) atoms. Note that in a 3 + 1 dimensional description, atoms are no longer discrete objects, but one-dimensional “atomic surfaces”. A particular section of the atomic surface results in the position of an atom in conventional 3D space. The electron density clearly shows how a particular position is dominated by Au in some regions and by Cd in others.

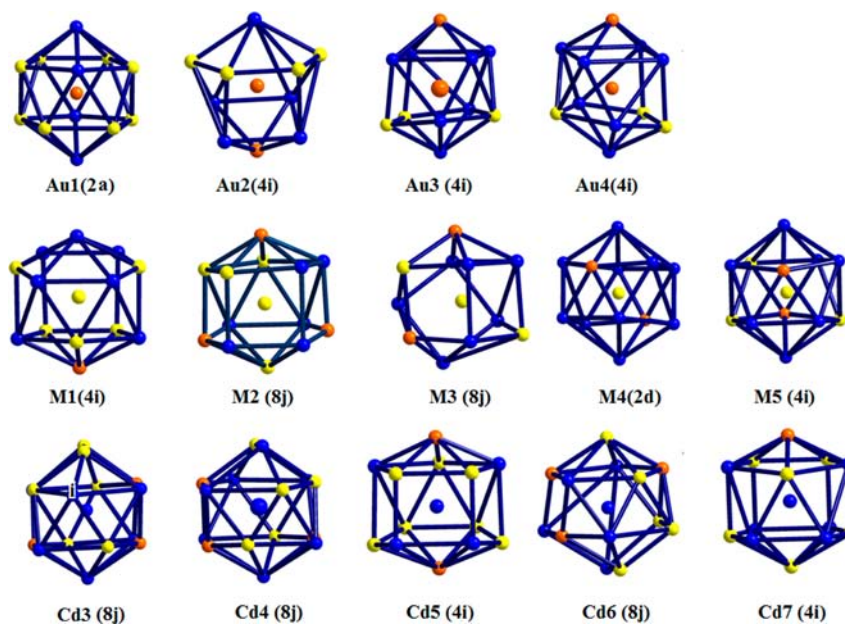


**Figure 5.** Coordination polyhedra of the atoms of the  $\text{AuCd}_{1.78}$  (C1) structure are shown. Constituting cadmium atoms are drawn in blue, pure gold in orange, and mixed gold/cadmium sites in yellow. Although the structure is modulated with respect to both occupancy and position, the latter effect is small and the polyhedra are relatively fixed in shape.

using occupational modulations. Au and Cd were set to fill each site completely via complementary occupation modulation, and the two atoms were constrained to have the same displacive modulation and the same thermal parameters. The result could be improved to  $R_{\text{obs}} = 6\%$  for all observed reflections ( $R_{\text{obs}} = 4\%$  for main reflections and  $R_{\text{obs}} = 13\%$  for first order satellites). These results could be further improved to  $R_{\text{obs}} = 3.97\%$  for all observed reflections ( $R_{\text{obs}} = 3.55\%$  for main reflections and  $R_{\text{obs}} = 5.51\%$  first order satellites) by introducing first order harmonic modulation waves for the anisotropic thermal displacement parameters of all atoms. A table with all relevant

parameters for the refinement is found in the Supporting Information.

Single crystals of nominal composition  $\text{Au}_{3.25}\text{Cd}_{5.75}$  (C1) are quite small and as a result the weak satellites cannot be integrated. In the supplementary data only the average structure is given. Generally, the amplitudes of the displacive modulations are quite small. A notable exception is the mixed position M4, and to some extent position M1.

The occupancy modulations on M1–M5 are shown in Figure 3 and Figure 4 where also the displacive modulations are obvious.

## DISCUSSION

It is remarkable that the reported  $\gamma$ -brass type structures of the  $\delta$ - and  $\delta'$ -phases are, at least superficially, quite different from that of the  $\delta''$ -phase. There are, however, similarities. The structure of the  $\delta''$ -phase is what might be termed a failed Frank–Kasper phase. It is largely tetrahedrally close packed, but there are a small number of interstices that are rather octahedral than tetrahedral. The same is true for many of the Zn rich phases with Fe, Co, and Ni, and this also includes the  $\gamma$ -brasses. The structures are described in terms of their coordination polyhedra (Figure 5). It is possible to identify extended structural fragments of the  $\delta''$ -phase that resemble that of  $\gamma$ -brass, but the cell content of the  $\delta''$ -phase (72 atoms) does not correspond to any simple multiple of that of the primitive cell of  $\gamma$ -brass (26 atoms) and it is difficult to envisage a plausible path of reconstruction from one to the other although the transition takes place unquenchably. This is also supported by the dramatically different powder patterns of the  $\gamma$ -brasses and that of  $\delta''$ -Au<sub>1+x</sub>Cd<sub>2-x</sub>.

The basic structure of Au<sub>1+x</sub>Cd<sub>2-x</sub> represents a new type that may be derived from that of CoZn<sub>13</sub> by crystallographic shear. By initially ignoring the elemental ordering and considering positions only, it is possible to identify slabs in the structure of CoZn<sub>13</sub> that in Au<sub>1+x</sub>Cd<sub>2-x</sub> correspond very well to infinite *ab*-slabs with a thickness of one unit cell along *c*. The two structures share a common [010]-direction while the [100] Au<sub>1+x</sub>Cd<sub>2-x</sub> corresponds to [102]<sub>CoZn13</sub>. In Figure 5, a slab of CoZn<sub>13</sub>, 2*a* × 5*c* is shown. The structure is overlaid with broad red and narrow blue stripes. The red stripes are slabs that correspond to the structure of Au<sub>1+x</sub>Cd<sub>2-x</sub>. The thin blue stripes between them indicate the regions that are excluded when the basic structure of Au<sub>1+x</sub>Cd<sub>2-x</sub> is generated from CoZn<sub>13</sub>. Red lines divide the strips into unit cells. For extra clarity, a white cell at the center of the image corresponds to a single unit cell of Au<sub>1+x</sub>Cd<sub>2-x</sub>. It is important to note that both the red Au<sub>1+x</sub>Cd<sub>2-x</sub> stripes and the excluded regions are symmetric with respect to the 2/*m* symmetry of the CoZn<sub>13</sub> structure. The loci of the preserved inversion centers are indicated by heavy black circles. Because of the preservation of the local symmetry of the Au<sub>1+x</sub>Cd<sub>2-x</sub> unit cells, the translational structure that results from joining them up retains the symmetry of the parent structure. The red unit cell vertex positions become additional centers of symmetry. The combined area of a red and a blue cell corresponds to three CoZn<sub>13</sub> cells (Figure 6).

The elemental decoration of the atomic positions is rather different in Au<sub>1+x</sub>Cd<sub>2-x</sub> compared to CoZn<sub>13</sub> (conf. Table 1). There are six distinct atomic positions in CoZn<sub>13</sub>, and these split into new positions in Au<sub>1+x</sub>Cd<sub>2-x</sub> according to patterns that depend on the symmetry of the position in the two different cells. This relationship is shown in the table below. Because of the excluded volume (blue), the total number of atomic positions in the Au<sub>1+x</sub>Cd<sub>2-x</sub> unit cell is somewhat less than three times the content of the CoZn<sub>13</sub> cell.

The structure of Au<sub>1+x</sub>Cd<sub>2-x</sub> does however feature the additional complication that it is incommensurately modulated. The displacive part of the modulation is slight, and the major effect comes from compositional variations. This is in perfect agreement with the total absence of second order satellites in the diffraction pattern.

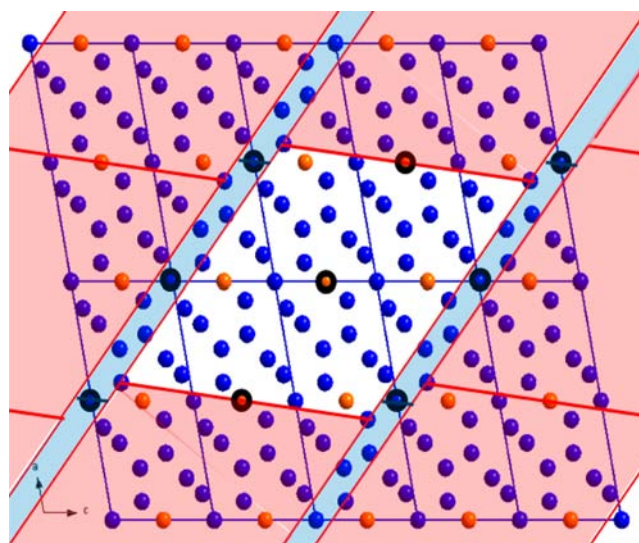


**Figure 6.** Column of CoZn<sub>13</sub>, 2*a* × ∞*b* × 5*c* is shown. The structure is overlaid with broad red and narrow blue stripes. The red stripes are slabs that correspond to the structure of Au<sub>1+x</sub>Cd<sub>2-x</sub>. The thin blue stripes between them indicate the regions that are excluded when the basic structure of Au<sub>1+x</sub>Cd<sub>2-x</sub> is generated from CoZn<sub>13</sub>. Red lines divide the strips into unit cells.

**Table 1. Comparison of the Decoration of CoZn<sub>13</sub> and Au<sub>1+x</sub>Cd<sub>2-x</sub>**

CoZn <sub>13</sub>	Wyckoff	Au <sub>1+x</sub> Cd <sub>2-x</sub>	Wyckoff
Co	2c	Au1	2c
		Au3	4i
Zn0	2a	M5	4i
		excluded	2x
Zn1	4i	Au2	4i
		Au4	4i
		Cd7	4i
Zn2	4i	M1	4i
		Cd5	4i
		excluded	4x
Zn3	8j	M4	2b
		Cd3	8j
		Cd6	8j
		excluded	2x
		excluded	4x
Zn4	8j	Cd4	8j
		M2	8j
		M3	8j
total	28 atoms in unit cell		72 atom in unit cell

## CONCLUSION

The compound  $\delta''$ -Au<sub>1+x</sub>Cd<sub>2-x</sub> (0.07 ≤ *x* ≤ 0.08) is synthesized, and the structure is determined by X-ray diffraction measurement. The structure of  $\delta''$ -Au<sub>1+x</sub>Cd<sub>2-x</sub> is incommensurately modulated, and the average structure represents a new structure type. The elemental ordering causes an incommensurate modulation. The structure of the  $\delta''$ -phase is almost tetrahedrally close packed. A small number of octahedral arrangements of atoms violate the tetrahedral close packing. The structure may be derived from that of  $\xi$ -CoZn<sub>13</sub> by crystallographic shear. The  $\delta''$ -phase is stable up to 652(1) K. A plausible path of reconstruction from  $\gamma$ -brass type  $\delta$ - and  $\delta'$ -phases to the  $\delta''$ -phase is not easy to establish, although the

transition takes place unquenchably. But it is evident that the  $\delta''$ -phase is completely different from that of reported the  $\delta$ - and  $\delta'$ -phases.

## ■ ASSOCIATED CONTENT

### ● Supporting Information

Rietveld profile fit, crystallographic and structural data, EDS formula, X-ray crystallographic files in CIF file format. This material is available free of charge via the Internet at <http://pubs.acs.org>.

## ■ AUTHOR INFORMATION

### Corresponding Author

\*E-mail: Partha.Jana@chem.lu.se. Fax: +46462224012. Phone: +46462224769.

### Notes

The authors declare no competing financial interest.

## ■ ACKNOWLEDGMENTS

The authors wish to thank VR, the Swedish National Science Research Council for the financial support.

## ■ REFERENCES

- (1) Westbrook, H. J.; Fleischer, L. R., Eds.; *Intermetallic Compounds: Principles and Practice*; John Wiley & Sons: Chichester, U.K., 1995; Vol. 1–2.
- (2) Villars, P.; Calvert, L. D. *Pearson's Handbook of Crystallographic data for Intermetallic Phases*, 2nd ed.; ASM International: Metals Park, OH, 1991.
- (3) Nesper, R. *Angew. Chem.* **1991**, *103*, 805–834; *Angew. Chem., Int. Ed. Engl.* **1991**, *30* (7), 789–817.
- (4) Miller, G. J. *Eur. J. Inorg. Chem.* **1998**, *5*, 523–536.
- (5) Lee, C.; Miller, G. J. *J. Am. Chem. Soc.* **2000**, *122*, 4937–4947.
- (6) Nesper, R. *Prog. Solid State Chem.* **1990**, *20*, 1–45.
- (7) Belin, C.; Thillard-Charbonnel, M. *Coord. Chem. Rev.* **1998**, *178–180*, 529–564.
- (8) Corbett, J. D. *Struct. Bonding (Berlin)* **1997**, *87*, 157–193.
- (9) Mizutani, U.; Takeuchi, T.; Sato, H. *Prog. Mater. Sci.* **2004**, *49*, 227.
- (10) Leisegang, T.; Meyer, Dirk, C.; Doert, T.; Zahn, G.; Weißbach, T.; Souptel, D.; Behr, G.; Paufler, P. *Z. Kristallogr.* **2005**, *220*, 128–134.
- (11) Otsuka, K. *Mater. Sci. Forum* **1990**, *56–58*, 393–404.
- (12) Nakanishi, N.; Mori, T.; Miura, S.; Murakami, Y.; Kachi, S. *Philos. Mag.* **1973**, *28*, 277–292.
- (13) Otsuka, K.; Shimizu, K. *Int. Met. Rev.* **1986**, *31*, 93.
- (14) Otsuka, K.; Wayman, C. M. In *Deformation behavior of materials*; Feltham, P., Ed.; Freund Publishing House: Tel Aviv, Israel, 1977; Vol. II, p 151.
- (15) Funakubo, H., Ed.; *Shape memory alloys*; Gordon Breach Science Publishers: New York, 1987.
- (16) Otsuka, K.; Wayman, C. M., Eds.; *Shape memory materials*; Cambridge University Press: Cambridge, U.K., 1998.
- (17) Nishiyama, Z. *Martensitic Transformations*; Academic Press: New York, 1978.
- (18) Christian, J. W. *The theory of transformations in metals and alloys*. Oxford: Pergamon Press, 1965.
- (19) Wayman, C. M. *Introduction to crystallography of martensitic transformations*; MacMillan: New York, 1964.
- (20) Warlimont, H.; Delaey, L. *Progress in Materials Science*; Pergamon Press: Oxford, U.K., 1974; Vol. 18.
- (21) Westgren, A.; Pharagmen, G. *Metallwirtschaft* **1928**, *7*, 702.
- (22) Olander, A. Z. *Kristallogr.* **1932**, *83*, 145–148.
- (23) Alasafi, K. M.; Schubert, K. J. *Less-Common Met.* **1977**, *51*, 225–233.

- (24) Alasafi, K. M.; Schubert, K. J. *Less-Common Met.* **1979**, *65*, 23–28.
- (25) Durrant, P. J. *J. Inst. Met.* **1929**, *41*, 139–171.
- (26) Komarek, K. L.; Stummerer, V. *Monatsh. Chem.* **1972**, *102*, 1360–1373.
- (27) Brown, P. J. *Acta Crystallogr.* **1962**, *15*, 608–612.
- (28) Petricek, V.; Dusek, M.; Palatinus, L. *Jana2006. The crystallographic computing system*; Institute of Physics: Praha, Czech Republic, 2006.
- (29) Palatinus, L.; Chapuis, G. J. *Appl. Crystallogr.* **2007**, *40*, 786–790.
- (30) Rietveld, H. M. *Acta Crystallogr.* **1967**, *22*, 151–152.
- (31) Rietveld, H. M. *J. Appl. Crystallogr.* **1969**, *2*, 65–71.